"Zipper" Molecular Beacons: A Generalized Strategy to Optimize the Performance of Activatable Protease Probes

ARTICLE *in* BIOCONJUGATE CHEMISTRY · SEPTEMBER 2009

Impact Factor: 4.51 · DOI: 10.1021/bc900207k · Source: PubMed

5 AUTHORS, INCLUDING:

Juan Chen
University Health Network
72 PUBLICATIONS **1,843** CITATIONS
SEE PROFILE

Pui-Chi Lo
The Chinese University of Hong Kong
56 PUBLICATIONS **1,454** CITATIONS
SEE PROFILE

Brian C Wilson
University of Toronto
341 PUBLICATIONS **8,146** CITATIONS
SEE PROFILE

COMMUNICATIONS

"Zipper" Molecular Beacons: A Generalized Strategy to Optimize the Performance of Activatable Protease Probes

Juan Chen, Tracy W. B. Liu,† Pui-Chi Lo, Brian C. Wilson, and Gang Zheng*

Department of Medical Biophysics, Ontario Cancer Institute, University of Toronto, Toronto, Ontario M5G 1L7, Canada.
Received May 7, 2009; Revised Manuscript Received August 31, 2009

We report the proof-of-principle concept for zipper molecular beacons (ZMB) comprising an asymmetrical polyarginine/polyglutamate electrostatic "zipper" hairpin-linked fluorophore−quencher pair. The objective is to balance maximal quenching efficiency and optimal two-step activation (protease cleavage/zipper dissociation), while enhancing target cell uptake. This strategy also eliminates the peptide sequence dependence of conventional protease beacons. This ZMB concept is a generalizable approach to improve the functionality of a wide range of diagnostic/therapeutic probes through a simple switching of substrate sequences.

INTRODUCTION

Optical molecular imaging has become a powerful tool for biochemical and cellular studies (*1*). With the continual development of peptide-based "smart probes", the *in vivo* optical imaging of specific molecular targets, biological pathways, and disease progression is gaining momentum. Many of the initial fluorescent probes had limited image contrast due to poor target specificity. Hence, activatable optical probes (*2*−*9*) that require enzyme-triggered separation of an inhibitory moiety from an active partner were developed. More recently, we and others have extended this concept to photodynamic molecular beacons (*10*−*14*) for increased specificity in photodynamic therapy. These activatable protease probes comprise an enzyme-specific linker with a fluorophore (or photosensitizer) and quencher conjugated at its opposite ends. The probes are inactive until the linker is cleaved by a target-specific enzyme. Although such activatable imaging and therapeutic beacons have shown great promise, several challenges have arisen.

First, the quenching depends on the natural peptide folding of the enzyme-specific linker. Thus, the probes are limited to sequences with natural conformations that bring the quencher and active moiety in close proximity in order for effective silencing to occur. In other words, different peptide sequences have different background fluorescence. A second concern is most protease-specific probes are activated extracellularly, so that the activated probes may diffuse to nontarget cells/tissues before target cell uptake occurs. Third, probes that target soluble proteases may be activated at sites distant from the target due to leakage of the enzyme from the target cells into the general circulation (*15*−*17*), thereby contributing to background signal and reduced contrast. Lastly, the probes use nonspecific/passive delivery to the target cells/tissues, which is suboptimal.

Recently, the concept of activatable cell-penetrating peptides (ACPP) was introduced to address the passive delivery of first-generation activatable optical probes. These are based on the electrostatic formation of a polycation/polyanion "zipper", whose linker can be selectively cleaved by a protease to locally unleash the delivery function of cell-penetrating peptides (CPP) (*15*−*17*). The underlying mechanism is functionally reminiscent of molecular beacons themselves that require enzyme-triggered separation of an inhibitory moiety from an active partner: here, the separation is between a polyanionic peptide (polyanion) and a polycationic peptide (polycation). Inclusion of a quencher may improve imaging contrast by suppressing the active partner before cleavage of the linker (*15*). The concept is illustrated in Scheme 1.

MATERIALS AND METHODS

All amino acid derivatives and the Sieber amide resin were purchased from Novabiochem (San Diego, CA, USA). The black hole quencher3 carboxylic acid succinimdyl ester (BHQ3-NHS) was obtained from Biosearch Technologies (Novato CA, USA). The pyropheophorbide carboxylic acid succinimidyl ester (Pyro-NHS) was prepared according to a published procedure (*18*). Other chemicals were obtained from Aldrich (Oakville, ON) and were used as received. Reverse-phase HPLC was preformed on a XBridgeTM-C8 column (2.5 μm, 4.6 × 150 mm) using a Waters 2695 controller with a 2996 photodiode array detector and a Waters ZQTM mass detector (Waters Limited, Mississauga, ON).

Synthesis of ZMB. The peptide sequence Fmoc-[D-Glu(Ot-Bu)]$_x$-protected activatable peptide linker-[D-Arg(Pbf)]$_y$Lys(Mtt) was synthesized on the Sieber resin according to a solid-phase peptide synthesis (SPPS) protocol using a PS3 peptide synthesizer (Protein Technologies) with commercially available *N*-α-Fmoc-protected amino acids. After the last Fmoc group had been removed from the peptide resin with 20% piperidine in *N*,*N*-dimethylformamide (DMF), the resin was washed with DMF. BHQ3-NHS was then coupled to the N-terminal of the peptide in DMF with *N*,*N*-diisopropylethylamine (DIPEA) (BHQ3/peptide = 3:1 molar ratio). The mixtures were shaken under argon overnight at room temperature. The acquired dark-blue resin was washed with DMF and then treated with 95%

* Correspondence to G. Zheng, TMDT 5-363, 101 College St, Toronto, ON M5G 1L7, Canada. Fax: 416-581-7666, gang.zheng@uhnres.utoronto.ca.
† First two authors contributed equally to this work.

10.1021/bc900207k CCC: $40.75
Published on Web 09/14/2009

Scheme 1. Universal Zipper Molecular Beacon Design[a]

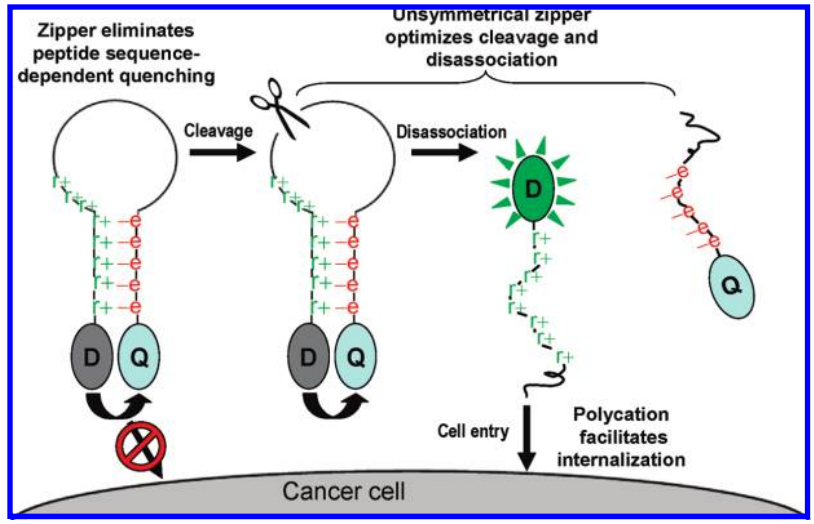

[a] The "zipper" is composed of a pair of polycation and polyanion arms holding the dye (D) and quencher (Q) in close proximity due to electrostatic attraction. This results in silenced dye activity independent of peptide linker variations. Upon specific enzymatic cleavage of the linker, the dye and quencher dissociate, resulting in dye photoactivity and unleashing the polycation, which increases cellular uptake.

trifluoroacetic acid (TFA) with 5% triisopropylsilane (Tis) to remove the protected groups on the peptide and cleave the peptide from the resin. After removing the solid support by filtration, the filtrates were concentrated and precipitated by diethyl ether to give the BHQ3-conjugated peptide, BHQ3-$_D$(e)x-activatable peptide linker-$_D$(r)yK(NH_2). The peptide was then reacted with Pyro-NHS in anhydrous DMSO with 1% DIPEA at ambient temperature for 6 h. The reaction mixture were then purified by HPLC to give pure BHQ3-$_D$(e)x-activatable peptide linker (r)yK(Pyro), which were characterized using UV−vis and ESI mass spectroscopy.

Synthesis of Controls. The synthesis of nonquencher control, Pyro-GPLGLARK (PP), and nonzipper control, Pyro-GPLGLARK-(BHQ3) (nonzip1), were reported previously (*12*). Nonzip2, Pyro-RPLALWRSK(BHQ3), was synthesized using the similar procedure as nonzip1. FITC-labeled polycation control, Fmoc-$_D$(r)x-K(FITC), was synthesized as follows: Fmoc-[D-Arg-(Pbf)]x-K(Mtt) was synthesized on the Sieber resin. The resin was then treated with 95% TFA with 5% Tis to remove the protected groups on the sequence and cleave the sequence from the resin. The acquired Fmoc-$_D$(r)x-K(ε-NH_2) was then reacted with fluorescein isothiocyanate (FITC) in anhydrous DMSO with 1% DIPEA at ambient temperature for 6 h. The reaction mixture were then purified by HPLC to give pure Fmoc-$_D$(r)x-K(FITC). Nonquencher ACPP control, Fmoc-$_D$(e)$_5$GPLGLA$_D$(r)$_8$K(Pyro) (Pyro-ACPP), was synthesized using a similar protocol to Fmoc-$_D$(r)x-K(FITC). The differences are in (1) replacing the peptide sequence and (2) conjugating Pyro-NHS on the C-terminal rather than FITC.

pH Dissociation Assay of ZMB. 0.5 μM of ZMB samples were prepared in adjusted PBS solutions with different pH (pH = 2, 3, 4, 5, 6, 7, 8, 9, 10, 11, 13). Their fluorescence emission was measured on a HORIBA FluoroMax-4 spectrofluorometer (excitation 650 nm, emission 675 ± 5 nm). Using the sample of pH = 7 as reference, the fluorescence increase in different pH conditions was calculated to evaluate the structure stability of ZMB.

Activation Studies. ZMB or nonzipper probes (1 nmol) were first dissolved in 2.5 μL of DMSO and 0.5 μL of Tween 80. The solution was diluted with 1 mL of phosphate-buffered saline (PBS) or minimum essential medium (MEM) Eagle cell media, and then incubated with 10 μL of human Proteinase K (2 μg) (ZMB/Proteinase K ~ 50:1 molar ratio). The activation was monitored by the fluorescence increase, which was calculated by normalizing the sample's fluorescence emission on real-time to its initial fluorescence. $FI_{protease}$ and FI_{TFA} were used to define the fluorescence increase at 2 h post-Proteinase K cleavage and following fluorescence increase after adding 1% TFA to the cleavage solution.

Evaluation of Polycation Delivery Capability. MT1 cells were grown to 60% confluence in Nunc Lab-TekII-CC2 chambered slides. Eagle's minimum essential medium (MEM) medium with 10% fetal bovine serum containing 5 μM of Fmoc-$_D$(rrrrr)-K(FITC) and Fmoc-$_D$(rrrrrrrr)-K(FITC) were added and incubated for 10 min at 37 °C. The cells were washed 3 times with PBS. The chamber slides were then imaged on an Olympus FluoView 1000 laser scanning confocal microscope equipped with a 488 nm argon laser.

Evaluation of Cell Uptake of ZMB before and after Activation. (1) Preparing nonactivation sample: Fresh MEM medium with 10% fetal bovine serum (without proteases) was used to prepare a 10 μM concentration of the probes. (2) Preparing postactivation samples: MT1 cells were grown in Nunc Lab-TekII-CC2 chambered slides for 3 days. A 10 μM concentration of the probes were prepared in this 3-day-old cell incubation medium (contains secreted proteases including MMP7) and incubated until the peptide linkers of probes were cleaved (monitored by HPLC). (3) Confocal study: 200 μL of these samples were incubated with MT1 cells in the chamber slides for 30 min. The chamber slides were washed with PBS 3 times and then imaged by a confocal microscope equipped with a 633 nm He−Ne laser.

RESULTS AND DISCUSSION

To test this concept, we designed a ZMB with four functional modules: (1) a protease cleavable peptide as the linker, (2) a polycation and a polyanion attached to each end of the linker, forming a "zipper" structure via electrostatic attraction, (3) pyropheophorbide as a fluorescent dye (D), and (4) a Black Hole Quencher 3 as a quencher (Q), conjugated to the end of the polycation and polyanion, respectively. As shown in Scheme 1, the zipper provides several potential advantages: (1) the formation of the polycation/polyanion "zipper" through electrostatic attraction improves the silencing of the beacon by bringing D and Q into closer contact, (2) a "hairpin" conformation of the substrate sequence occurs as a result of the zipper,

Table 1. Abbreviations of Protease Probes

probe	sequence
nonzip1	Pyro-GPLGLARK(BHQ3)
nonzip2	Pyro-RPLALWRSK(BHQ3)
zipXe	BHQ3-$_D$(e)$_X$GPLGLA$_D$(r)$_X$K(Pyro)
zip8e2	BHQ3-$_D$(e)$_8$ RPLALWRS$_D$(r)$_8$K(Pyro)
zip5e8r	BHQ3-$_D$(e)$_5$ GPLGLA$_D$(r)$_8$K(Pyro)
PP	Pyro-GPLGLARK

improving the cleavage rate of the enzyme-specific linker, (3) the polyanionic arm of the zipper prevents the probe from entering cells, by blocking the cell-penetrating function of the polycation, (4) the polycationic arm enhances cellular uptake of the dye after linker cleavage, and (5) quenching is no longer dependent upon the natural folding of the peptide linker, since the zipper is solely responsible for the "dormant" state. In the presence of a target protease, the peptide linker is first specifically cleaved; the Q-attached polyanion then dissociates from the D-attached polycation, becoming photoactive, and unleashes the polycation, which enhances the delivery of the activated dye locally into the target cells.

In order to examine the effect of the zipper conformation on the photophysical properties, two matrix metalloproteinase 7 (MMP7)-specific peptide sequences, GPLGLARK (*19*) and RPLALWRSK (*20*), were used to synthesize two ZMBs, zip8e and zip8e2, and their corresponding nonzipper controls, nonzip1 and nonzip2 (see Table 1). Eight consecutive D-arginines, $_D$(rrrrrrrr), and D-glutamates, $_D$(eeeeeeee), were selected as the polycation and polyanion, respectively, as these can assemble into a stable zipper hairpin structure (*15*). D-Amino acids were used for the zipper arms, since they are stable against proteolysis (*21*). Also, D-amino acid-based polycationic peptides present similar cell penetrating capabilities to the natural L-amino acids (*22*).

The fluorescence emission of these probes was evaluated, normalized to that of the nonquencher probe, PP. As shown in Figure 1C, a marked difference in the fluorescence of nonzip1 and nonzip2 was observed (<2% and 27.2%, respectively). There was only a slight difference in the length and solubility of the peptide linkers in nonzip1 and nonzip2, indicating that the fluorescence quenching efficiency in the nonzipper probes does depend on the natural folding of the linkers (Supporting Information Figure S1 and Table S1, HPLC retention time). However, with the inclusion of the zipper, the quenching efficiencies were enhanced, with the fluorescence of zip8e and zip8e2 being reduced to 0.4% and 0.9%, respectively. This comparable quenching in zip8e and zip8e2 indicates that the quenching dependence on the natural folding of the peptide linker has been eliminated. Moreover, in aqueous solution, the specific absorption peaks of Pyro (414 nm) and BHQ3 (676 nm) in zip8e were shifted relative to their corresponding nonzipper probes (nonzip1) (Figure 1A). By adjusting the solution to a low pH condition (pH = 2) to neutralize the polyanion sequence and unfold the peptide sequence, the fluorescence of zip8e was increased 4-fold and its specific absorption was restored (Figure 1B), while nonzip1 did not show any obvious changes. Therefore, the enhanced quenching efficiency in the ZMB is presumably the result of both the improved fluorescence resonance energy transfer (FRET) effect and the ground-state complex quenching (contact quenching) caused by annealing D and Q through the electrostatic attraction of the zipper arms.

We next verified the electrostatic nature of the zipper conformation using a pH dissociation assay. As shown in Figure 1D, the fluorescence values of both zip8e and nonzip1 were very stable at pH ~ 5−9. At pH < 5, the fluorescence of zip8e increased continually with decreasing pH, while that of nonzip1 was unchanged. This suggests that the zipper conformation disassociates at pH around 4, coinciding with the isoelectric point of the glutamic acid, and so confirming the electrostatic nature of the zipper conformation. The fluorescence increase at pH ≥ 10 observed in zip8e and nonzip1 is due to decomposition of BHQ3.

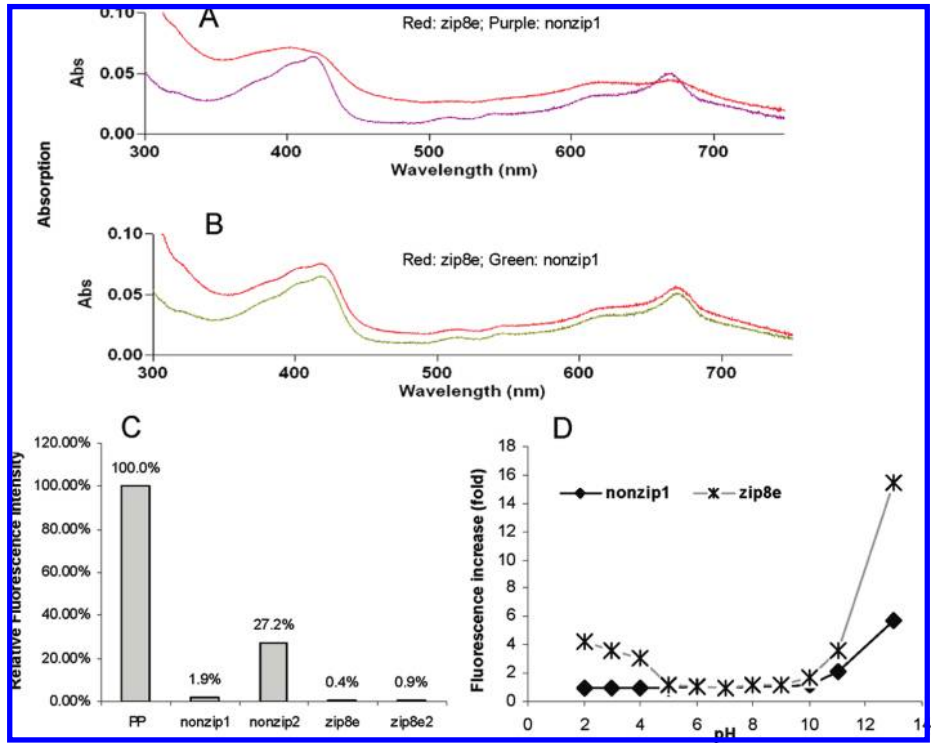

Figure 1. (A) Absorption spectra of zip8e and nonzip1 in (A) PBS buffer and (B) low-pH solution (pH = 2). (C) Relative fluorescence intensity of protease activatable probes (normalized to the fluorescence emission of PP). (D) The fluorescence stability of zip8e and nonzip1 in PBS buffer in the pH range 2−13.

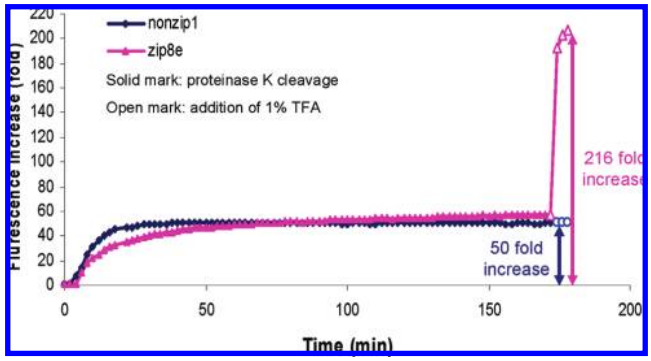

Figure 2. Comparison of the protease-mediated activation of ZMB and nonzipper probes: Cleavage kinetic profiles of probes depict increase in fluorescence after 3 h protease incubation and post TFA-induced disassociation.

Examining the protease-triggered activation of ZMB (Figure 2), we determined that the activation of ZMB is a two-step process. The first step is cleavage of the peptide linker and the second is dissociation of the zipper arms. Kinetic cleavage profiles of zip8e and nonzip1 were evaluated using Protease K to ensure complete proteolysis of the linker, and upon achieving stable fluorescence intensity, trifluoroacetic acid (TFA) was added. This decreased the pH to 2, neutralizing the polyanion arm and consequently causing dissociation of the zipper to produce maximum fluorescence. Both the nonzip1 and zip8e constructs were completely cleaved by Protease K in 3 h and produced similar maximum fluorescence. However, the fluorescence increases of these two probes were significantly different due to the enhanced quenching efficiency afforded by the zipper mechanism. As shown in Figure 2, nonzip1 resulted in a 50-fold fluorescence increase due to proteolysis with no further fluorescence increase after the addition of 1% TFA. In contrast, zip8e produced an overall 216-fold fluorescence increase. However, only a 57-fold fluorescence increase was observed 3 h after proteolysis and a 159-fold increase was contributed by forced dissociation of the zipper arms after the addition of 1% TFA. These results demonstrate that ZMB activation is a two-step process. When compared with the nonzip1 construct, ZMB offers much higher signal/background ratio after activation (216-fold vs 50-fold) due to a lower fluorescence background of intact ZMB, generated by zipper-enhanced fluorescence quenching.

This two-step activation creates a dilemma that is also observed in activatable cell-penetrating peptide probes in which the liberation of the peptide has a different mechanism on a much slower time scale (*15*). On one hand, a stable zipper conformation is necessary to achieve maximum quenching efficiency, which is critical for improving the probe sensitivity (by reducing the background fluorescence) and for creating the sequence-independent universal probe. On the other hand, if the zipper structure is too stable, it prevents or slows the prompt dissociation of the D- and Q-zipper arms upon target activation. This results in nonspecific diffusion of D from the target cells and diminishes the gain in probe selectivity. Hence, the optimal ZMB should have a high quenching efficiency balanced by rapid dissociation of the zipper arms after proteolysis.

Although zip8e provides near-maximum quenching efficiency (99.6%), its activation only produces a partial fluorescence increase (26%) from general proteolysis. In order to balance the quenching efficiency and activation, a collection of ZMBs with different zipper arm lengths (zip3e, zip4e, zip5e, zip6e) were synthesized (Supporting Information Figure S1 and Table S1). By comparing their fluorescence emission in PBS buffer, we found that the longer the zipper arm (polycation/ polyanion pair), the greater the quenching efficiency (Figure 3A). Upon

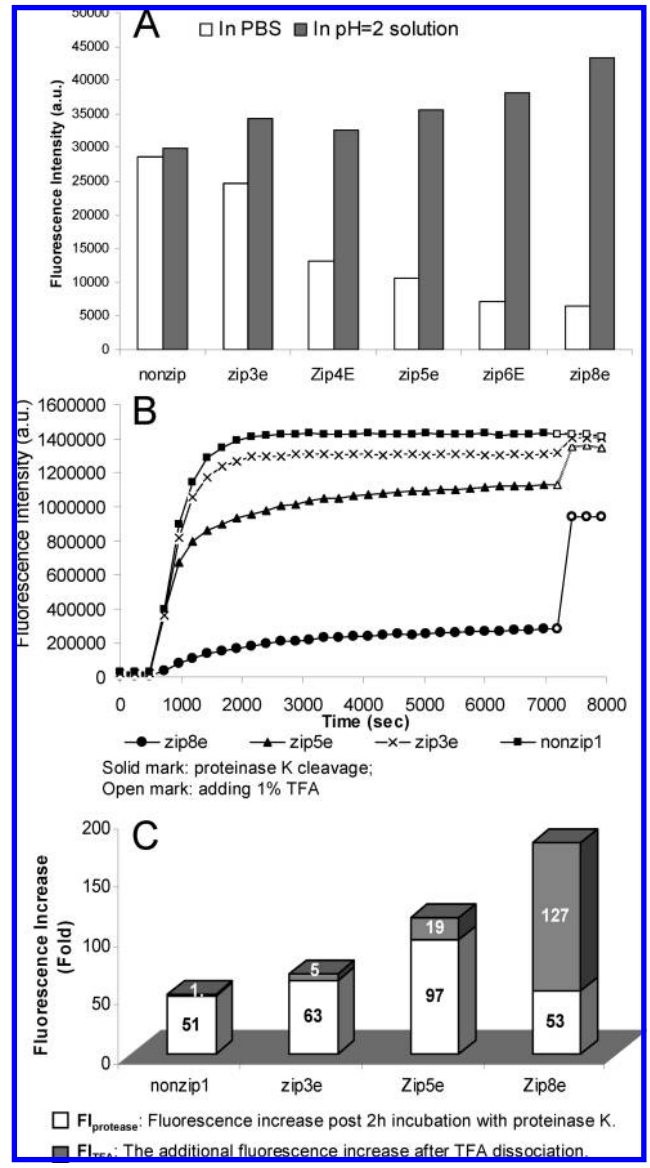

Figure 3. (A) Fluorescence emission of intact ZMBs in PBS and low pH condition (pH = 2). (B) Protease cleavage monitored by real time fluorescence. (C) $FI_{protease}$ and FI_{TFA} values for ZMBs and nonzipper controls.

adjusting the pH to 2, little to no fluorescence increase was observed in zip3e, suggesting that a zipper structure was not formed in this molecule, while a significant fluorescence increase, due to the low pH condition, was observed in zip4e, zip5e, zip6e, and zip8e, indicating that a zipper structure was formed in these molecules. The low pH conditions neutralize the polyanionic arm eliminating the electrostatic attraction between the zipper arms causing dissociation. This results in fluorescence release, as the D and Q are no longer electrostatically held together in close proximity.

As seen in Figure 3B, the activation of zip3e and zip5e was compared with that of nonzip1 and zip8e upon Proteinase K cleavage. Zip3e showed similar activation kinetics as nonzip1, further indicating that a 3-amino acid zipper arm length does not form a stable zipper. It had been previously observed that the 4-glutamate motif does not effectively attenuate the translocation of CPPs prior to proteolytic cleavage (*17*). Thus, these characteristics suggest that a stable zipper is formed when the ZMB is composed of more than 4 consecutive polycations and polyanions, resulting in enhanced fluorescence quenching efficiency and the two-step activation process. In Figure 3C, a

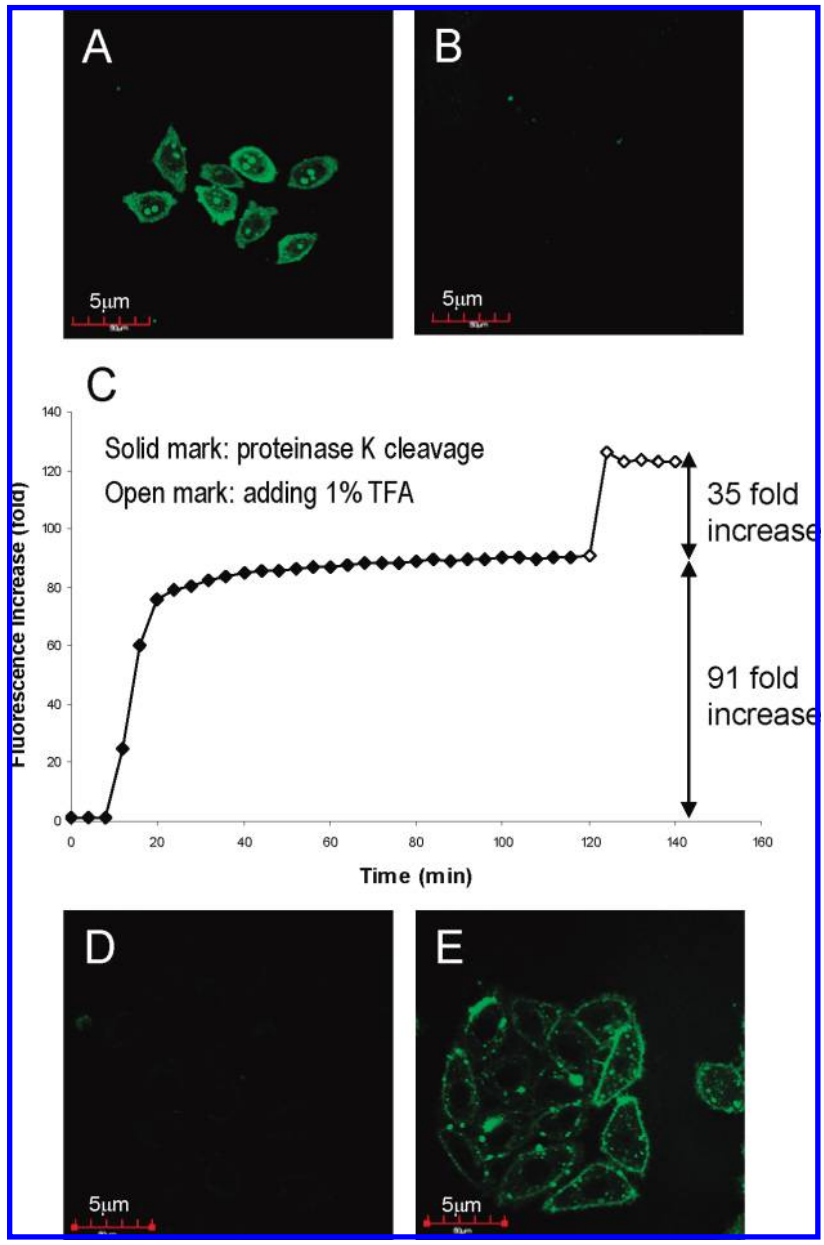

Figure 4. Confocal images of 5 μM (A) Fmoc-$_D$(rrrrrrrr)-K(FITC) and (B) Fmoc-$_D$(rrrrr)-K(FITC) in MT1 cells showing fluorescence in each case. (C) Activation kinetics of zip5e8r by Proteinase K in PBS. Confocal images of cell uptake of (D) nonzip1 and (E) zip5e8r at 30 min after cleavage by 3-day-old MT1 cell culture media.

97-fold fluorescence increase was seen in zip5e after proteolysis of the peptide linker ($FI_{protease}$), while only a 19-fold increase occurred after addition of TFA (FI_{TFA}). Thus, the dissociation of the zipper arms in zip5e is a much more efficient process than that of zip8e.

As all of the above fundamental studies were performed in PBS solution, we further evaluated the stability of the zipper arms in cell culture MEM media. Although the dissociation of the zipper arms is slightly increased in different buffered conditions, a 3−5% increase in fluorescence occurred; we assume that this buffer change will not greatly influence the kinetic profile of the zip PMBs (Supporting Information Figure S3).

Although zip5e has optimal cleavage and zipper arm dissociation rates, the practicality of a 5-amino acid polycation arm assisting in the internalization of the fluorophore is questionable. It has been reported that effective cell penetration requires at least 6 consecutive cationic amino acids (*23*). To validate this, *in vitro* confocal fluorescence microscopy was performed on Fmoc-$_D$(rrrrr)-K(FITC) and Fmoc-$_D$(rrrrrrrr)-K(FITC). As shown in Figure 4A,B, the 5-consecutive arginine cannot deliver the FITC into cells, whereas the 8-consecutive arginine showed a rapid uptake, within both the cytoplasm and nucleus after only 10 min incubation. This should address the limitation of nonspecific diffusion of the probe upon extracellular activation. Thus, by combining the optimal activation (cleavage and dissociation) of zip5e with the strong cell penetrating ability of 8-consecutive arginines, we designed an asymmetric ZMB with 8-consecutive arginines and 5-consecutive glutamates (zip5e8r): BHQ3-$_D$(eeeee)GPLGLA$_D$(rrrrrrrr)K(Pyro). This produces almost identical fluorescence quenching efficiency as zip5e (99.4% vs 99.3%), a similar rate of cleavage (2 h to completion) (Figure 4C) and comparable overall activation (72% vs 84%).

On the basis of these positive findings, zip5e8r was further evaluated in MT1 breast carcinoma cells *in vitro*, comparing the cell delivery of nonzip1 and zip5e8r after activation by 3-day-old cell incubated media. Although the peptide linker sequence is considered MMP7-specific (*12*), the old cell media

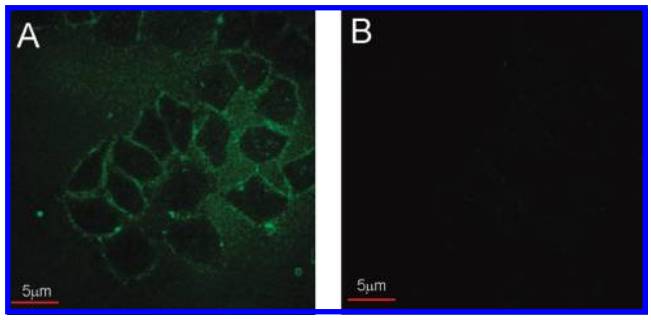

Figure 5. Confocal images comparing the background fluorescence in Pyro-ACPP (A) and zip5e8r (B).

contains a variety of different proteases, which might also lead to beacon activation. As shown in Figure 4D,E, the cleaved moiety of 8-consecutive arginine with Pyro (8r-Pyro) after zip5e8r activation accumulated inside the cells within 30 min, while the nonzip1 showed very weak uptake after activation. The improvement of zip5e8r ZMB over the corresponding nonquencher ACPP control, Pyro-ACPP, is shown in Figure 5 and Supporting Information Figure S5. By confocal imaging of the uptake of zip5e8r and Pyro-ACPP in fresh cell culture media and 3-day-old cell incubation media, we observed that the addition of a quencher significantly decreased the background signal, both before and after probe cleavage. Thus, ZMBs increased the resolution of activated probes and the contrast between the intact and activated beacon.

In summary, encoding a suitable zipper structure into protease-activatable probes significantly improves their functionality. First, by forming a stable zipper conformation, protease probes with different quenching efficiency can reach comparable maximum values (99.6% for zip8e and 99.1% for zip8e2). This effectively eliminates the peptide substrate sequence dependence of the quenching. Second, an optimal balance between high quenching efficiency and rapid activation (protease cleavage + zipper dissociation) can be achieved with 5-consecutive arginine paired with 5-consecutive glutamate (for both zip5e and zip5e8r). However, only the asymmetric zip5e8r with the extended polyarginine arm can facilitate rapid cell internalization. Thus, by incorporating an asymmetric zipper control, the quenching efficiency, activation, and delivery can all be optimized simultaneously, and the probe is no longer dependent on the specific peptide substrate sequence. Consequently, by simply switching the substrate sequences, the ZMB design can potentially be applied to a wide range of protease probe applications, with predictably similar functional performance.

This ZMB design has universal applications in targeted cancer fluorescence imaging/diagnostics, since in principle, any tumor biomarker can be targeted. Future advances may rely upon ZMBs targeted to novel early and reliable tumor markers that can discriminate malignant from benign lesions and detect micrometastases at distant sites. The application of ZMBs in cancer therapeutics is achievable by simply switching D to a fluorescent photosensitizer, such as pyropheophorbide. The ZMBs will then possess novel targeting capabilities for photodynamic therapy (PDT). With the activatable nature of ZMBs, another level of PDT selectivity should be achievable, improving the accuracy and reliability of this noninvasive therapeutic technique. Furthermore, with the fluorescent production upon activation of ZMBs, a "see and treat" approach in cancer therapeutics is also possible. The novelty of the ZMB construct is that it provides a universal design for any combination of Q and D or photosensitizer and any disease biomarker target. Thus, the applications of activatable molecular beacons in cancer diagnosis and therapy can be expanded with the incorporation of the "zipper" mechanism.

ACKNOWLEDGMENT

This work was supported by the Canadian Institute of Health Research, the Ontario Institute for Cancer Research through funding provided by the Government of Ontario, the Canadian Cancer Society Research Institute, and the Joey and Toby Tanenbaum/Brazilian Ball Chair in Prostate Cancer Research.

Supporting Information Available: Characterization of ZMB constructs, confirmation of protease K cleavage fragments of ZMBs, comparison of the fluorescence emission and kinetic profile of zip5e and zip8e in buffer solutions, comparison of ACPP vs ZMB in vitro after cleavage. This material is available free of charge via the Internet at http://pubs.acs.org.

LITERATURE CITED

(1) Weissleder, R., and Ntziachristos, V. (2003) Shedding light onto live molecular targets. *Nat. Med. 9*, 123–8.
(2) Weissleder, R., Tung, C. H., Mahmood, U., and Bogdanov, A. (1999) In vivo imaging of tumors with protease-activated near-infrared fluorescent probes. *Nat. Biotechnol. 17*, 375–8.
(3) McIntyre, J. O., Fingleton, B., Wells, K. S., Piston, D. W., Lynch, C. C., Gautam, S., and Matrisian, L. M. (2004) Development of a novel fluorogenic proteolytic beacon for in vivo detection and imaging of tumour-associated matrix metalloproteinase-7 activity. *Biochem. J. 377*, 617–628.
(4) Bullok, K., and Piwnica-Worms, D. (2005) Synthesis and characterization of a small, membrane-permeant, caspase-activatable far-red fluorescent peptide for imaging apoptosis. *J. Med. Chem. 48*, 5404–5407.
(5) Blum, G., von Degenfeld, G., Merchant, M. J., Blau, H. M., and Bogyo, M. (2007) Noninvasive optical imaging of cysteine protease activity using fluorescently quenched activity-based probes. *Nat. Chem. Biol. 3*, 668–677.
(6) Jaffer, F. A., Kim, D., Quinti, L., Tung, C., Aikawa, E., Pande, A. N., Kohler, R. H., Shi, G., Libby, P., and Weissleder, R. (2007) Optical visualization of cathepsin K activity in atherosclerosis with a novel, protease-activatable fluorescence sensor. *Circulation 115*, 2292–2298.
(7) Melancon, M. P., Wang, W., Wang, Y., Shao, R., Ji, X., Gelovani, J. G., and Li, C. (2007) A novel method for imaging in vivo degradation of poly(L-glutamic acid), a biodegradable drug carrier. *Pharm. Res. 24*, 1217–1224.
(8) Zhang, Z., Yang, J., Lu, J., Lin, J., Zeng, S., and Luo, Q. (2008) Fluorescence imaging to assess the matrix metalloproteinase activity and its inhibitor in vivo. *J. Biomed. Opt. 13*, 011006.
(9) Stefflova, K., Chen, J., Marotta, D., Li, H., and Zheng, G. (2006) Photodynamic therapy agent with a built-in apoptosis sensor for evaluating its own therapeutic outcome in situ. *J. Med. Chem. 49*, 3850–6.
(10) Chen, J., Stefflova, K., Niedre, M. J., Wilson, B. C., Chance, B., Glickson, J. D., and Zheng, G. (2004) Protease-triggered photosensitizing beacon based on singlet oxygen quenching and activation. *J. Am. Chem. Soc. 126*, 11450–1.
(11) Choi, Y., Weissleder, R., and Tung, C. (2006) Selective antitumor effect of novel protease-mediated photodynamic agent. *Cancer Res. 66*, 7225–7229.
(12) Zheng, G., Chen, J., Stefflova, K., Jarvi, M., Li, H., and Wilson, B. C. (2007) Photodynamic molecular beacon as an activatable photosensitizer based on protease-controlled singlet oxygen quenching and activation. *Proc. Natl. Acad. Sci. U.S.A. 104*, 8989–94.
(13) Gabriel, D., Campo, M. A., Gurny, R., and Lange, N. (2007) Tailoring protease-sensitive photodynamic agents to specific disease-associated enzymes. *Bioconjugate Chem. 18*, 1070–1077.
(14) Lo, P., Chen, J., Stefflova, K., Warren, M. S., Navab, R., Bandarchi, B., Mullins, S., Tsao, M., Cheng, J. D., and Zheng,

G. (2009) Photodynamic molecular beacon triggered by fibroblast activation protein on cancer-associated fibroblasts for diagnosis and treatment of epithelial cancers. *J. Med. Chem. 52*, 358–368.

(15) Jiang, T., Olson, E. S., Nguyen, Q. T., Roy, M., Jennings, P. A., and Tsien, R. Y. (2004) Tumor imaging by means of proteolytic activation of cell-penetrating peptides. *Proc. Natl. Acad. Sci. U.S.A. 101*, 17867–72.

(16) Goun, E. A., Shinde, R., Dehnert, K. W., Adams-Bond, A., Wender, P. A., Contag, C. H., and Franc, B. L. (2006) Intracellular cargo delivery by an octaarginine transporter adapted to target prostate cancer cells through cell surface protease activation. *Bioconjugate Chem. 17*, 787–96.

(17) Watkins, G. A., Jones, E. F., Scott Shell, M., VanBrocklin, H. F., Pan, M., Hanrahan, S. M., Feng, J. J., He, J., Sounni, N. E., Dill, K. A., Contag, C. H., Coussens, L. M., and Franc, B. L. (2009) Development of an optimized activatable MMP-14 targeted SPECT imaging probe. *Bioorg. Med. Chem. 17*, 653–9.

(18) Zhang, M., Zhang, Z., Blessington, D., Li, H., Busch, T. M., Madrak, V., Miles, J., Chance, B., Glickson, J. D., and Zheng, G. (2003) Pyropheophorbide 2-deoxyglucosamide: a new photosensitizer targeting glucose transporters. *Bioconjugate Chem. 14*, 709–14.

(19) Knight, C. G., Willenbrock, F., and Murphy, G. (1992) A novel coumarin-labelled peptide for sensitive continuous assays of the matrix metalloproteinases. *FEBS Lett. 296*, 263–6.

(20) Welch, A. R., Holman, C. M., Browner, M. F., Gehring, M. R., Kan, C. C., and Van Wart, H. E. (1995) Purification of human matrilysin produced in *Escherichia coli* and characterization using a new optimized fluorogenic peptide substrate. *Arch. Biochem. Biophys. 324*, 59–64.

(21) Hamamoto, K., Kida, Y., Zhang, Y., Shimizu, T., and Kuwano, K. (2002) Antimicrobial activity and stability to proteolysis of small linear cationic peptides with D-amino acid substitutions. *Microbiol. Immunol. 46*, 741–9.

(22) Gammon, S. T., Villalobos, V. M., Prior, J. L., Sharma, V., and Piwnica-Worms, D. (2003) Quantitative analysis of permeation peptide complexes labeled with Technetium-99m: chiral and sequence-specific effects on net cell uptake. *Bioconjugate Chem. 14*, 368–76.

(23) Mitchell, D. J., Kim, D. T., Steinman, L., Fathman, C. G., and Rothbard, J. B. (2000) Polyarginine enters cells more efficiently than other polycationic homopolymers. *J. Pept. Res. 56*, 318–25.

BC900207K